Electron Transfer within Charge-Localized Arylhydrazine-Centered Mixed Valence Radical Cations Having Larger Bridges

Stephen F. Nelsen* and Kevin P. Schultz

Department of Chemistry, University of Wisconsin, 1101 University Avenue, Madison, Wisconsin 53706-1396

Received: December 26, 2008; Revised Manuscript Received: March 14, 2009

Kinetics for intramolecular charge transfer between two diarylhydrazine units, measured by ESR, are reported for six charge-localized mixed valence compounds having 9, 11, 13, and 16 bonds between the nitrogen atoms. A 17-bond bridged compound had too slow electron transfer to measure the rate constant by ESR. The optical spectra of these radical cations are compared with tert-butyl,aryl-substituted hydrazines, and rate constants calculated using parameters derived from the optical spectra are compared with the experimental values where possible. The charge-transfer band overlapped too badly with bridge-centered absorption for the 16-bond bridged compound to allow the comparison to be made. The 13-bond bridged compound gave worse agreement than the other compounds. Its optical rate constant was about 5.4 times the ESR rate constant at a temperature between the ranges in which the data were collected.

Introduction

The simplest mixed valence (MV) compounds have two charge-bearing units (CBUs, **M**) attached to a bridge (**B**) and are at an oxidation level that is an odd number so that the charges on the CBUs might be different, and they are radical ions.[1−3] The concept was devised for transition-metal coordination complexes that have one bivalent ligand bridging the metals, but this paper concerns all-organic examples. When the charge is mostly localized on one **M** group, so that a radical cation example would be usefully considered to be $\mathbf{M^0-B-M^+}$ (called a Robin−Day class II system),[1] these are the most revealing electron-transfer (ET) systems known because of Hush theory.[3] We initially became interested in hydrazine-centered MV compounds to test Hush's remarkably simple evaluation of both the reorganization energy (λ, equal or close to the band maximum transition energy, $\bar{\nu}_{max}$) and the electronic coupling H_{ab}, given by eq 1,[3] from the charge-transfer band absorption spectrum of class II compounds (for energies in cm^{-1} and the electron distance d_{ab} in Å)

$$H_{ab} = 0.0206(\bar{\nu}_{max}\Delta\bar{\nu}_{1/2}\varepsilon_{max})^{1/2}/d_{ab} \quad (1)$$

$\Delta\bar{\nu}_{1/2}$ is the full width at half-height, and ε_{max} is the extinction coefficient in $M^{-1}cm^{-1}$. For this purpose we used **HytBu** (see Chart 1) as the **M** groups when aromatic bridges were employed and measured electron-transfer rate constants using electron spin resonance (ESR).[4−11] These studies showed that the λ and H_{ab} values calculated using Hush theory predict the electron-transfer rate constants remarkably well and that agreement with experiment is improved by minor adjustments to Hush's method, including a refractive index correction to ε_{max} and changing the way in which d_{ab} is estimated. In this work, we have examined larger bridges, which required increasing the rate constants from those obtained using **M** = **HytBu** to keep them in the range measurable by ESR, near 10^8 sec^{-1}. We have done so by employing aryl third substitutents at nitrogen, **HyPh** or **HyAn**, which has been shown to substantially lower λ_v[9,12] and also raise H_{ab} because there is less twisting at the CN bonds connecting the substituents to the bridge; therefore, the rate constants are significantly larger than those for **HytBu**-substituted examples. We recently discussed results showing that **HyAr**-centered radical cations having 5- and 7-atom aromatic bridges are charge-delocalized (Robin−Day class III) compounds and that the biphenyl-bridged compound is charge-localized in acetonitrile.[13]

Chart 2 shows the structures of the bridges referred to in this paper. There has been considerable study and discussion of the optical spectra of **Sti**- and **Tol**-bridged MV radical cations having the dianisylamino charge-bearing unit $\mathbf{An_2N}$,[14−19] to which data on bis(hydrazines) under discussion will be compared. We will describe these bridges using *n*, the number of bonds between the closest nitrogen atoms. In addition to the 11-bond bridges, the $n = 13$ bond dihexyl-oxyterphenyl bridged (**DHT**) compound, the $n = 16$ bridged ethylenedioxythiophene-linked bis(phenylethynyl) (**EDOT**) compound, and the $n = 17$ bond bridged dihexyloxybenzene-linked bis(phenylethynyl) (**PEDT**) compound were examined to see if special effects caused by relatively low-lying bridge radical cations would result. Such an effect has been observed for the five-bond bridged $\mathbf{(HytBu)_2}$ radical cation with a $^{\mathbf{910}}$**AN** bridge.[20] Compounds with smaller bridges, several of which are delocalized, were described separately.[13]

Experimental Section

Generation of the Radical Cations in Methylene Chloride and Acetonitrile. ***Method 1.*** The neutral compound was dissolved in a small amount of MC (distilled over CaH_2). The silver salt used ($AgSbF_6$ or $AgPF_6$) was weighed out under a nitrogen atmosphere and added as a MC solution to the neutral compound. It was stirred for at least 20 min and then was filtered through a syringe filter (0.2 μm) into a 10.00 mL volumetric flask and diluted to the mark with MC. Then, using a volumetric pipet, a known amount (usually a 1.00 or 2.00 mL aliquot) of MC solution was transferred into a new 10.00 mL volumetric flask, and several milliliters of AN was added while under nitrogen purge. The contents were purged until the volume decreased significantly, and then again, AN was added. After at least 1 h of strong purging, the solution was diluted to the

* To whom correspondence should be addressed.

10.1021/jp811433p CCC: $40.75
Published on Web 04/17/2009

CHART 1: Charge-Bearing Units, M

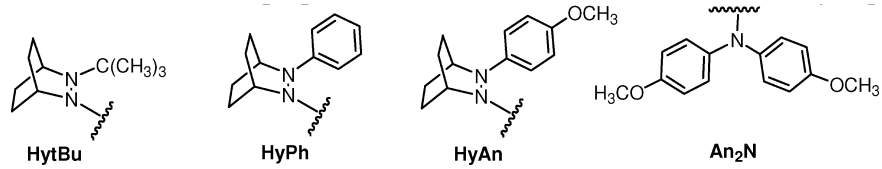

CHART 2: Structures of the Bridges Discussed Here

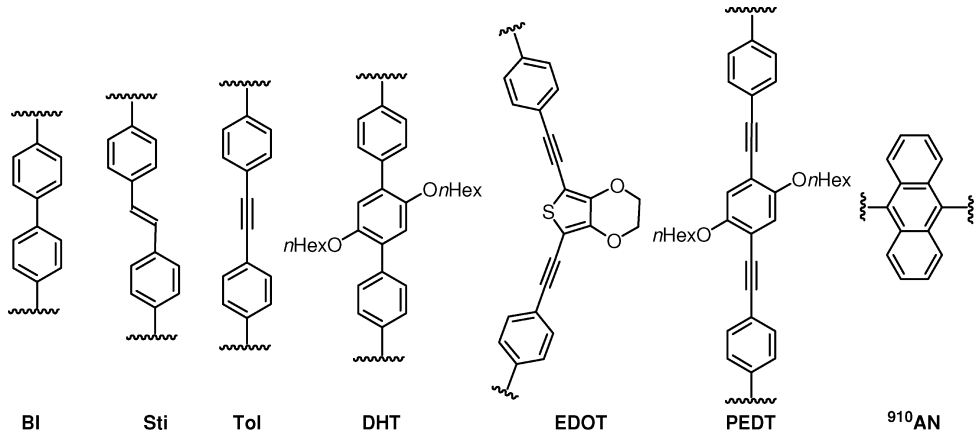

TABLE 1: Rate constants Determined by ESR in PrCN

$(HyPh)_2BI\text{-}d_{10}^+$		$(HyAn)_2Tol\text{-}d_8^+$		$(HyPh)_2Tol\text{-}d_{18}^+$		$HyAn_2Sti\text{-}d_{10}^+$	
T (K)	k_{ESR}	T (K)	k_{ESR}	T (K)	k_{ESR}	T (K)	k_{ESR}
204	0.94×10^8	313	1.43×10^8	275	9.62×10^7	216	1.18×10^8
207	1.05×10^8	316	1.56×10^8	279	1.06×10^8	219	1.32×10^8
210	1.27×10^8	319	1.67×10^8	285.5	1.18×10^8	222	1.45×10^8
214	1.47×10^8	322	1.82×10^8	290	1.32×10^8	228	1.75×10^8
218	1.70×10^8			300	1.59×10^8	234	2.08×10^8
				308	1.89×10^8		

mark, and it was now a pure AN solution. Each solution could then be diluted further if necessary to obtain the optical concentration, which was about 0.05−0.2 mM. An optical spectrum of the original MC solution was taken initially and then concurrently with the AN solution to ensure stability of the radical cation.

Method 2. If the stability of the radical cation did not allow for Method 1, the neutral compound was dissolved in the appropriate solvent. If it did not dissolve, then it was sonicated for several hours. Next, tris(*p*-bromophenyl)aminium hexachloroantimonate (E_{red} = 1.1V versus SCE)[21] was weighed out and dissolved in the appropriate solvent. The oxidant solution was then added to the neutral compound solution and stirred for 10−15 min. The optical spectrum was taken immediately. The reduced triarylamine does not absorb light in the region of interest or show an ESR signal. The aminium cation is reasonably stable for long periods of storage and is soluble in many organic solvents, which makes it a useful oxidant for organic systems.[22]

Intramolecular ET Rate Constants. The rate constants determined by simulations of the ESR spectra in this work appear in Tables 1 and 2.

Results and Discussion

Compound Preparation. As in previous work, the bis(hydrazines) were prepared by adding bis(lithio) salts of the aromatic bridge, prepared from brominated aromatic compounds, to suitably substituted diazenium cations. The dibromotolane necessary for preparation of **Tol** bridges was made by Sonagashira coupling of *p*-bromoiodobenzene with acetylene,[23] and the dibromostilbene for **Sti** bridges was made by Wittig coupling of the phosphonium salt from *p*-bromobenzyl bromide with *p*-bromobenzaldehyde, followed by refluxing with a trace of iodine to convert the product mixture to *trans*-dibromostilbene.[24] Because the ESR spectra were too broad for accurate simulation for all protio materials, dibromotolane-d_8 was prepared from benzene-d_6, and the dilithium salt was added to phenyldiazonium-d_5 salt $\mathbf{2b}^+$, prepared as in Scheme 1, to produce $(HyPh)_2Tol\text{-}d_{18}$.

TABLE 2: Rate Constants Determined by ESR in 1,2-Dichloroethane

$(HyPh)_2DHT\text{-}d_{10}^+$	
T (K)	k_{ESR}
304	1.149×10^8
310	1.266×10^8
316	1.449×10^8
324	1.667×10^8
330	1.818×10^8

SCHEME 1: Preparation of the Aryldiazonium Salts

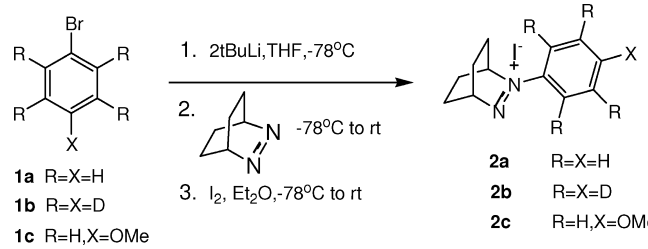

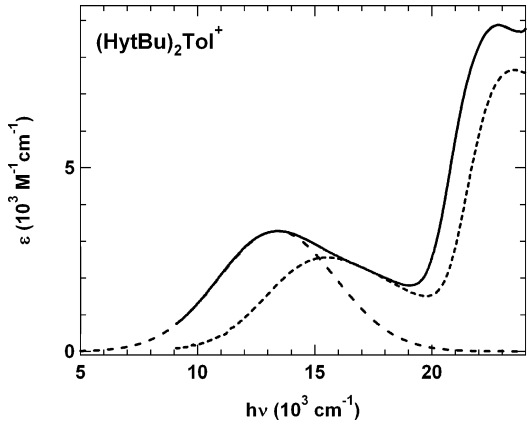

Figure 1. Optical spectra of **(HytBu)$_2$Tol**$^+$ in methylene chloride (solid line) and acetonitrile (short dashed). Long dashed line is a Gaussian fit.

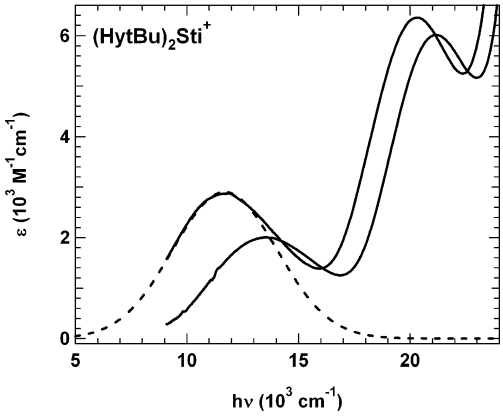

Figure 2. Optical spectra of **(HytBu)$_2$Sti**$^+$, as that in Figure 1.

When we failed to find conditions that would hydrogenate **HyPh$_2$Tol** to the stilbene-bridged compound, we prepared dibromostilbene-d_{10} via a McMurray coupling of deuterated benzaldehyde[25] and subsequently **(HyAn)$_2$Sti-*d*$_{10}$** by adding its dilithio compound to **2c**.

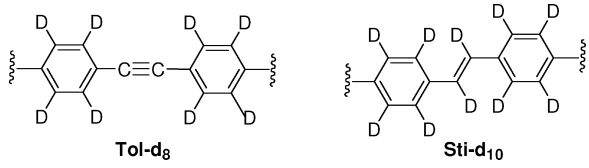

The $n = 13$ dihexyloxyterphenyl compound **(HyPh)$_2$DHT** was synthesized using Suzuki coupling of the dihexyloxydiboronic acid[26] with four equivalents of 1,4-bromoiodobenzene to yield the dibromodihexyloxyterphenyl (**DHT**) bridge, which was coupled to the diazonium salt. The longer bridges containing acetylenes, **(HyPh)$_2$EDOT** and **(HyPh)$_2$PEDH**, were made using Sonogashira chemistry[27−29] to obtain the dibromides, which were subsequently coupled to the diazonium salt. For details, see the Supporting Information. In all cases, the deuterated **HyPh-*d*$_5$** units were employed for the compounds reported here, but for brevity, we will not mention the deuteration again in this paper.

Optical Spectra. The optical spectra of the 9−13-bond MV compounds first described here are compared in AN and MC solvents in Figures 1−8.

Tables 3−5 summarize optical data on **(HytBu)$_2$B**$^+$, **(HyPh)$_2$B**$^+$, and **(HyAn)$_2$B**$^+$ in MC and AN for the compounds now available.

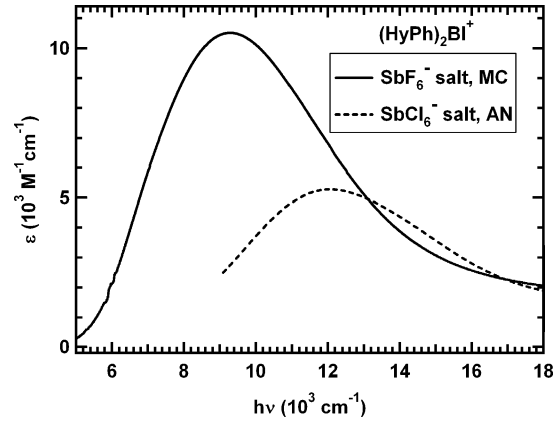

Figure 3. Optical spectra of **(HyPh)$_2$BI**$^+$, as that in Figure 1.

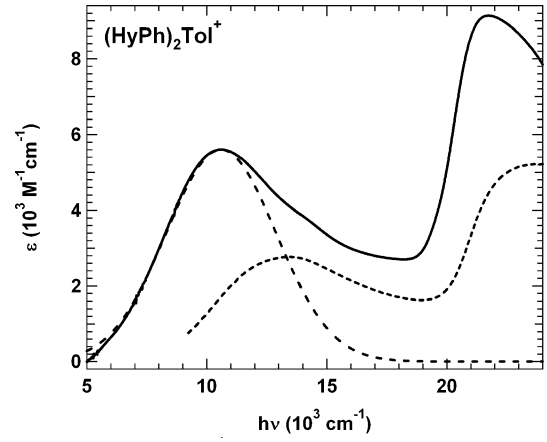

Figure 4. Optical spectra of **(HyPh)$_2$Tol**$^+$, as that in Figure 1.

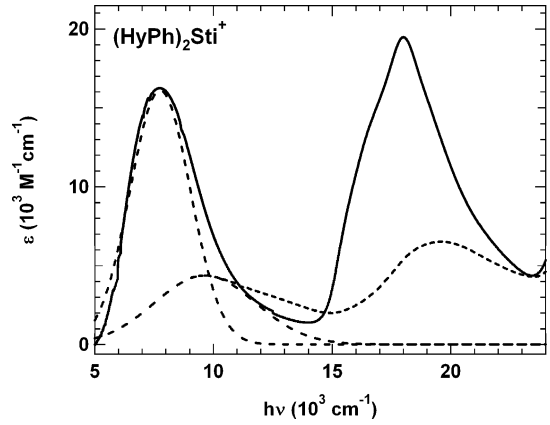

Figure 5. Optical spectra of **(HyPh)$_2$Sti**$^+$, as that in Figure 1.

***λ* and *ε*$_{max}$ Values.** The **HytBu**-centered compounds studied for the 9- and 11-bond bridges are clearly localized. The ET rate constants for the **BI**-bridged compound have been measured by ESR in both MC and AN,[7,8] and both the **Tol**- and **Sti**-bridged ones only exhibit slow ET on the ESR time scale. For class II compounds, $\bar{\nu}_{max} = \lambda$ if parabolic diabatic surfaces are employed[3] and is close to λ if this assumption is relaxed.[6] Because $\lambda = \lambda_v + \lambda_s$, one needs to consider the sizes of both of these quantities to understand how $\bar{\nu}_{max}$ changes in class II compounds. We shall first consider estimation of λ_v from calculations. Calculation of λ_v values for MV compounds is more difficult than that for intermolecular electron-transfer reactions because of technical problems. Hartree−Fock calculations give very poor geometries for hydrazine radical cations presumably because they ignore electron correlation and,

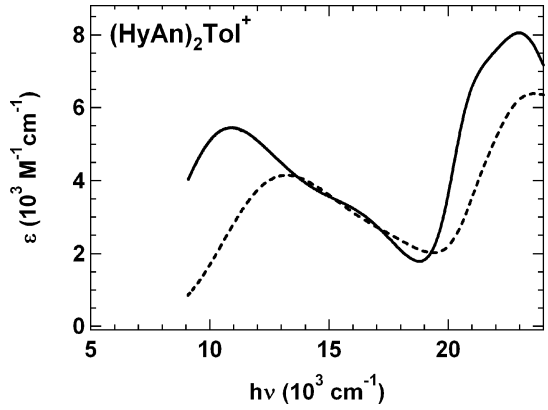

Figure 6. Optical spectra of **(HyAn)$_2$Tol**$^+$, as that in Figure 1.

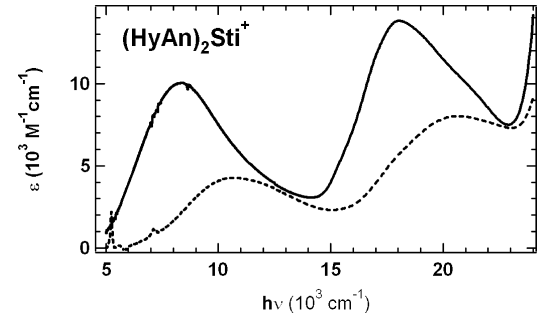

Figure 7. Optical spectra of **(HyAn)$_2$Sti**$^+$, as that in Figure 1.

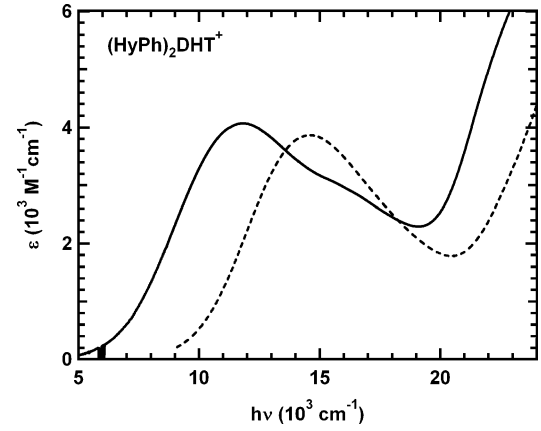

Figure 8. Optical spectra of **(HyPh)$_2$DHT**$^+$ in MC and AN.

probably as a result, give greater geometry changes upon electron loss than actually occur, causing considerable overestimation of λ_v values.[30] B3LYP hybrid HF-DFT calculations get much better geometries for monohydrazines but basically do not know about mixed valency because they overestimate the importance of electron delocalization, which causes them to get the geometries nearly the same at both **HytBu** groups of class II MV compounds, causing them to greatly underestimate λ_v for them. Because electronic interactions through the bridge mix the character of the oxidized and neutral **M** groups, as may be seen in the X-ray structures of two **(HytBu)$_2$B**$^+$ MV compounds,[5] calculation of the enthalpy contribution to λ_v for monohydrazine analogues of the MV compounds with a phenyl group replacing the bridge should give an upper limit that corresponds to the value expected for low H_{ab} compounds and to intermolecular reactions, where H_{ab} is rather low. Although we rather loosely called the **HyR** group the "charge-bearing unit" in counting the number of bonds between the closest nitrogens, it is clear that much charge is delocalized on both of the aryl groups of **HyAr** in these compounds. The calculations used what is sometimes called the four-point method,[31] which has been successfully applied to the interpretation of intermolecular electron-transfer rate constants using calculations at the B3LYP/6-31+G* level;[11] the results are shown in Table 6.

The $\bar{\nu}_{max}$ observed for **(HytBu)$_2$PH**$^+$ is 10800 cm^{-1} in MC, which is slightly smaller than the calculated value for only λ_v of **HytBuPh**$^{0/+}$ in Table 4,[5] illustrating the decrease in λ_v that occurs because of mixing of the character of the oxidized and neutral **M** groups through the bridge in MV compounds; this one has a relatively large H_{ab} value of ~2200 cm^{-1}.[8] The lowering caused by H_{ab} ought to be smaller for the larger bridged systems, but the numbers in Table 4 are expected to be at least slightly larger than those for MV systems.

Turning to the solvent reorganization energies, λ_s for class II MV radical cations is significantly larger in AN than that in MC; therefore, $\Delta\bar{\nu}_{max} = [\bar{\nu}_{max}(AN) - \bar{\nu}_{max}(MC)]$ is always positive and is observed to be in the range of 1900−3100 cm^{-1} for compounds discussed here (Tables 1−3). We note that the total λ values for **HyAn**-centered compounds are higher than those for **HyPh**-centered ones, instead of being lower, as is calculated for λ_v of **HyAnPh**$^{0/+}$ (Table 4). We suggest that this occurs because better solvation of the anisyl groups raises their λ_s values relative to **HyPh**-centered compounds. The regular increase in $\bar{\nu}_{max}$ with the number of bonds in the bridge for the **HyPh**-centered compounds in AN that is expected from the increase in λ_s as bridge size increases using dielectric continuum theory is seen for the **BI**, **Tol**, and **DHT** bridges, but all three **Sti**-bridged compounds have smaller $\bar{\nu}_{max}$ in both solvents despite slightly larger distances. It is known from previous work on hydrazine-bridged MV radical cations that dielectric continuum theory does a rather poor job of predicting their λ_s values because, among other things, it ignores the solvation energy of the bridge, which is not negligible for these compounds, and because specific interactions with solvent that do not correlate with the reciprocal of the refractive index squared minus the reciprocal of the static dielectric constant are not included.[8] The difference between the **Sti** and **Tol** bridges is the two carbon atom link between the aryl groups. A significant factor raising λ_s for this type of compound is the electron-donating ability of the solvent,[8] which we suggest leads to a significantly larger λ_s for the acetylene link (C≡C) of the **Tol** bridge than that for the vinyl (CH═CH) link of the **Sti** bridge. The sp-hybridized carbons of C≡C are more electronegative than the sp^2-hybridized ones of CH═CH, probably causing larger specific solvation effects, and the extra hydrogen atoms of **Sti** might inhibit (CH═CH) link solvation relative to **Tol**.

It has often been assumed that $\bar{\nu}_{max} = 2H_{ab}$ for class III compounds.[14−17,32] Using this equation assumes that the transition observed corresponds to the energy gap in a single two-state model. This cannot be the case for these compounds because as is well-known[16,17] that the intense and narrower transitions observed in class III compounds are between molecular orbitals of different symmetries, and MOs of different symmetries do not split each other. As we have pointed out in collaboration with Zink and co-workers, at least three diabatic energies and two electronic couplings are required to determine $\bar{\nu}_{max}$ for class III MV compounds of the type under discussion.[33−36] Although none of the $\bar{\nu}_{max}$ values show very large deviations from what is expected if all represent λ values for class II compounds, it may be noted that the **Sti**-bridged compounds have smaller $\Delta\bar{\nu}_{max}$ values than the **Tol**-bridged ones and that the amount depends upon the fourth hydrazine substituent, the value for the **Sti**-bridged compound being 86% as large as

TABLE 3: Comparison of Optical Spectra for $(HytBu)_2B^+$ Mixed Valence Compounds

		in CH_2Cl_2 (MC)			in MeCN (AN)				
B	bonds betw. Ns	$\bar{\nu}_{max}(\varepsilon_{max})$	$\Delta\bar{\nu}_{1/2}$	$\Delta\bar{\nu}_{1/2}$[b] ratio	$\bar{\nu}_{max}(\varepsilon_{max})$	$\Delta\bar{\nu}_{1/2}$	$\Delta\bar{\nu}_{1/2}$[b] ratio	$\Delta\bar{\nu}_{max}$[c]	$\Delta\varepsilon_{max}$[d]
BI	9	13000(2650)	6270	1.15	15200(2600)	6090	1.03	2200	50
Sti	11	11700(2900)	5500	1.06	13600(2000)	5300	0.95	1900	900
Tol	11	13400(29100)	5900	1.06	15600(2260)	6100	1.02	2200	700

[a] Ratio of the high-energy half-width at half-height to the low-energy half-width at half-height. [b] Ratio of the observed $\Delta\bar{\nu}_{1/2}$ to the Hush minimum value for a class II compound using parabolic diabatic surfaces (eq 2). [c] $\bar{\nu}_{max}$ (AN) − $\bar{\nu}_{max}$ (MC). [d] ε_{max}(MC) − ε_{max}(AN).

TABLE 4: Comparison of Optical Spectra for $(HyPh)_2B^+$ Mixed Valence Compounds

		in CH_2Cl_2 (MC)			in MeCN (AN)				
B	bonds betw. Ns	$\bar{\nu}_{max}(\varepsilon_{max})$	$\Delta\bar{\nu}_{1/2}$	$\Delta\bar{\nu}_{1/2}$[a] ratio	$\bar{\nu}_{max}(\varepsilon_{max})$	$\Delta\bar{\nu}_{1/2}$	$\Delta\bar{\nu}_{1/2}$[a] ratio	$\Delta\bar{\nu}_{max}$[c]	$\Delta\varepsilon_{max}$[d]
BI	9	9300(10500)	6650	1.43	12000(5300)	7000	1.33	2700	5200
Sti	11	7700(18100)	3520	**0.84**	9700(5500)	5300	1.06	2000	12600
Tol	11	10200(5300)	6230	1.3	13100(3800)	~7600[e]	~1.4	2900	1500
DHT	13	11500(4500)	5700	1.1	14600(3800)	~7800	~1.7	3100	700

[a] Ratio of the high-energy half-width at half-height to the low-energy half-width at half-height. [b] Ratio of the observed $\Delta\bar{\nu}_{1/2}$ to the Hush minimum value for a class II compound using parabolic diabatic surfaces (eq 2). [c] $\bar{\nu}_{max}$ (AN) − $\bar{\nu}_{max}$ (MC). [d] ε_{max}(MC) − ε_{max}(AN). [e] Overlaps on the high-energy side; only estimates available.

TABLE 5: Comparison of Optical Spectra for $(HyAn)_2B^+$ Mixed Valence Compounds

		in CH_2Cl_2 (MC)			in MeCN (AN)				
B	bonds betw. Ns	$\bar{\nu}_{max}(\varepsilon_{max})$	$\Delta\bar{\nu}_{1/2}$	$\Delta\bar{\nu}_{1/2}$[a] ratio	$\bar{\nu}_{max}(\varepsilon_{max})$	$\Delta\bar{\nu}_{1/2}$	$\Delta\bar{\nu}_{1/2}$[a] ratio	$\Delta\bar{\nu}_{max}$[c]	$\Delta\varepsilon_{max}$[d]
Sti	11	8400(10000)	5200	1.2	10700(4300)	~6600[e]	~1.3	2300	5700
Tol	11	11000(4780)[e]	7300[e]	1.4[e]	>13700(2000)	~8000[e]	~1.4[e]	2700	2780

[a] Ratio of the high-energy half-width at half-height to the low-energy half-width at half-height. [b] Ratio of the observed $\Delta\bar{\nu}_{1/2}$ to the Hush minimum value for a class II compound using parabolic diabatic surfaces (eq 2). [c] $\bar{\nu}_{max}$ (AN) − $\bar{\nu}_{max}$ (MC). [d] ε_{max}(MC) − ε_{max}(AN). [e] Overlaps on the high-energy side; only estimates available.

the **Tol**-bridged one for the **HytBu**-centered systems, 85% as large for the **HyAn**-centered ones, but only 69% as large for the **HyPh**-centered ones.

We next consider the ε_{max} values of Tables 3−5. It is well established experimentally that ε_{max} values increase significantly when charge delocalization occurs by decreasing bridge size using the same charge-bearing units.[16,17] Because the **HytBu**-centered compounds are localized, their ε_{max} values should depend roughly upon H_{ab}^2 (see eq 1), which in most cases makes ε_{max} slightly higher in MC than that in AN because $\bar{\nu}_{max}$ is smaller in MC and H_{ab} does not change. We note that $(HytBu)_2BI^+$, where the measured ε_{max} was larger in AN, is an exception to this expectation and that the discrepancy is not very large. The very large increase in ε_{max} in MC for $(HyPh)_2Sti^+$ is striking. The ε_{max} value changes more for the **Sti**-bridged than the **Tol**-bridged systems and is sensitive to the fourth substituent on the hydrazine, $\Delta\varepsilon_{max}$ being 78% as large for **Tol**-bridged as for **Sti**-bridged for the strongly trapped **HytBu**-centered pair, 49% for the **HyAn**-centered pair, but only 12% for the **HyPh**-centered pair. The large increase in ε_{max} for $(HyPh)_2Sti^+$ is accompanied by a decrease in bandwidth to a value significantly smaller than the Hush-predicted minimum for a class II compound; see eq 2.

$$\Delta\bar{\nu}_{1/2}(\text{min}) = (16RT\ln(2)\bar{\nu}_{max})^{1/2} \quad (2)$$

The ratios of observed $\Delta\bar{\nu}_{1/2}$ to $\Delta\bar{\nu}_{1/2}$(min) are shown in Tables 1−3, where it will be noted that all of the other entries round to 1.0 or greater (we note here that overlap of the CT band to which eq 2 refers with bridge excitation in the tolane-bridged systems probably makes the bandwidth observed larger than it should be). Similar data for the five- and seven-bond bridged **HyAr** compounds previously studied and assigned as delocalized show many ratios below 1.0.[13] As do Barlow and co-workers for a similar increase in ε_{max} and decrease in bandwidth for $(An_2N)_2Sti^+$ in MC,[16,17] we rationalize these optical spectrum changes as resulting from charge delocalization in the low λ_s solvent MC but not in the higher λ_s AN. We do not, however, attribute the reason for delocalization for **Sti**-bridged but not **Tol**-bridged compounds to an unusually large H_{ab} for the former (because we do not accept that $\bar{\nu}_{max} = 2H_{ab}$ for delocalized compounds) but to the significantly larger λ_s for the tolane-bridged compound.

TABLE 6: Calculated λ'_v Values for Monohydrazines at (U)B3LYP (in cm^{-1})

couple	λ'_v(6-31G*)[a]	λ'_v(6-31+G*)[a]	$\Delta\lambda'_v$
$HytBuPh^{0/+}$	10900[a]	10500[a]	[≡ 0]
$HyPh_2^{0/+}$	9600[a]	9300[a]	−1200
$HyAnPh^{0/+}$	8800[b]	est. 8500	est. −2000

[a] From ref 11. [b] This work.

Ion Pairing. MV bis(hydrazine) radical cations are ion-paired in MC, which makes their optical spectra somewhat sensitive to concentration because $\Delta G°$ for electron transfer is not 0 for the ion-paired form, as it is for the free ion in solution, causing $\bar{\nu}_{max}$ to increase as concentration and, hence, the fraction of ion-paired material present increase.[8,37,38] Ion-pairing effects have not been detected in the more polar AN. The data reported in Tables 3−5 are for concentrations that give a convenient absorption intensity in a 1 cm cell. Ion-pairing studies similar to those previously carried out were done for three of the compounds studied here, and analysis of the data is included in Table 6. As before, a fit to a simple ion pairing equilibrium, $[A^+] + [X^-] \rightleftarrows [AX]$, was satisfactory (see the equations used and plots of the fits in Supporting Information). Although the statistical error to the fits to $\bar{\nu}_{max}$(free) and $\bar{\nu}_{max}$(IP) is shown in Table 7, the actual error is larger, estimated at about ±100

TABLE 7: Ion Pairing Results for Aromatic-Bridged Mixed Valence bis(Hydrazines) in MC (but for $(HyPh)_2DHT^+SbF_6^-$, 1,2-dichloroethane)

compound	K_{IP} M^{-1}	$\Delta G°_{IP}$ kcal/mol	$\bar{\nu}_{max}$(free) cm^{-1}	$\bar{\nu}_{max}$(IP) cm^{-1}	$\Delta G°_{ET,IP}$ kcal/mol
$(HytBu)_2DU^+PF_6^-$ [a]	3100 ± 1000	−4.7 ± 0.2	12400	13100	2.0
$(HytBu)_2BI^+$ PF_6^- [a]	~3100 ± 1000	−4.7 ± 0.2	12900	13800	2.6
$(HyPh)_2BI^+$ SbF_6^- [b]	6500 ± 1400	−5.2 ± 0.2	8950 ± 14	10000 ± 50	3.0 ± 0.1
$(HyPh)_2Tol^+$ SbF_6^- [b]	7700 ± 1000	−5.3 ± 0.2	10000 ± 10	11000 ± 30	2.9 ± 0.1
$(HyPh)_2DHT^+SbF_6^-$ [b]	~4600 ± 1200	−5.0 ± 0.2	11420	11860	1.3 ± 0.1

[a] Ref 37. [b] This work.

TABLE 8: Eyring Activation Parameters for Aryl-Bridged Dihydrazine Radical Cations

compound	solvent	bnd	T range	$\Delta H^‡$ kcal/mol	$\Delta S^‡$ cal/(mol K)	$\Delta G^{‡a}$(260 K)	rel. k_{260}[a]
$HytBu_2BI^+$	MeCN	9	328−353	3.4_8 ± 0.13	−10.9 ± 0.4	6.31 ± 0.02	0.39
$(HyPh)_2BI^+$	PrCN	9	204−218	3.4 ± 0.5	−4.6 ± 2.3	4.61 ± 0.07	10.8
$(HyAn)_2Sti^+$	PrCN	11	216−234	2.7 ± 0.1	−8.5 ± 0.4	4.90 ± 0.02	6.2
$(HyAn)_2Tol^+$	PrCN	11	313−322	4.62 ± 0.7	−6.6 ± 2.1	6.33 ± 0.12	0.39
$(HyPh)_2Tol^+$	PrCN	11	275−308	2.8 ± 0.2	−11.5 ± 0.6	5.84 ± 0.02	≡1
$(HyPh)_2DHT^+$	$(CH_2Cl)_2$	13	304−330	3.0 ± 0.3	−11.9 ± 0.9	6.07 ± 0.15	0.64
$(HyPh)_2EDOT^+$	CH_2Cl_2	16	250−280	2.2 ± 0.2	−12.9 ± 0.7	5.54 ± 0.01	1.8

[a] Calculated at 260 K from the Eyring parameters, relative to $(HyPh)_2Tol$ (at 6.68×10^7 s^{-1}).

cm^{-1}.[39] The difference between $\bar{\nu}_{max}$(free) and $\bar{\nu}_{max}$(IP) allows calculation of the increase in free energy for electron transfer within the ion-paired species, shown in the last column as $\Delta G°_{ET,IP}$. Although the larger separation of the charge-bearing units and changes in their structure cause larger $\Delta G°_{IP}$ values for the **Tol**-bridged compounds than those found in previous work, the more important parameter for considering the ET rate constant, $\Delta G°_{ET,IP}$, is not detectably higher than for the five-bond bridged compound. Furthermore, the 13-bond bridged DHT bridge produces smaller $\Delta G°$ values for ion pairing than the 11-bond **Tol** bridge presumably because the average position of the counterions is closer to the center of the molecule than that for the **Tol** bridge.[8] The effects of ion pairing on electron-transfer rate constants for these compounds are perhaps surprisingly small and will not be further discussed here.

ESR Kinetics. Kinetics of intramolecular ET were measured by variable-temperature ESR and fit with a program that includes anisotropic line broadening effects for nitrogen, modified by J. P. Telo (T.U. Lisboa) from one written by Shohoji.[40−42] The rate constants must lie rather close to 10^8 s^{-1} to be measured accurately because the spectrum is only sensitive to temperatures near the nitrogen splitting constant in MHz. Because the reactivity of the tolane- and stilbene-bridged systems could only be compared directly for the $HyAn_2$-centered compounds and differ so much that they require a large difference in temperature for the rate constant measurements, we used butyronitrile as the solvent for these studies; therefore, the solvent would at least be the same. Bridge deuteration was required to narrow the spectra enough for reasonable accuracy in the rate constant measurements. Sample fits for $(HyPh)_2Tol^+$ are shown in Figure 9, where it may be seen how sensitive the spectra are to temperature near $k_{ESR} = 10^8$ s^{-1}; the ratio of rate constants used for the two fits is 1.96. Unfortunately, $(HyPh)_2Sti^+$ proved to have k_{ESR} slightly too high to measure accurately; therefore, we switched to the **HyAn** charge-bearing unit to be able to directly compare the **Tol**- and **Sti**-bridged compounds. This switch of the aryl group lowered k_{ESR} enough to make the measurement. The solvent chosen for the ESR kinetic comparisons was butyronitrile. A rather wide range of temperatures was necessary to get k_{ESR} into the measurable range (near 10^8 s^{-1}); therefore, to facilitate comparison, we compare the Eyring parameters determined in this work with earlier data for **HytBu**-centered systems[7,8] and compare calculated rate constants at a common temperature in Table 8. The 17-bond bridged $(HyPh)_2PEDT^+$ only showed the five line pattern for slow electron transfer on the ESR time scale in methylene chloride; therefore, its rate constant proved too small to measure presumably because this bridge is significantly twisted at the Ar−Ar bond, which lowers H_{ab}.

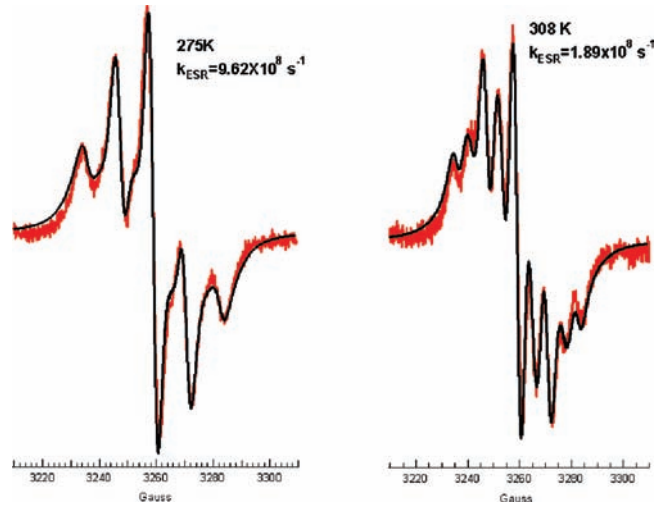

Figure 9. Fits to the ESR spectra for $(HyPh)_2Tol^+$ at 275 and 308 K.

Although no one thinks that the Eyring pre-exponential factor is appropriate for electron-transfer reactions, so that the $\Delta S^‡$ values do not represent realistic entropy values, comparisons of the relative values are appropriate. As is often the case, large and compensating values of $\Delta H^‡$ and $\Delta S^‡$ are observed for $(HyAn)_2Tol^+$ relative to the other examples, causing concern about the accuracy of the separation of entropy and enthalpy effects in this case. Figure 10 shows Eyring plots for the data first reported here. It may be seen that the **HyAn** CBU gives a slightly higher barrier than **HyPh** for the tolane-bridged systems (so the useful range for obtaining ESR rate constants occurs at higher temperature, further left on the plot). The methoxy substitution of the **HyAn**-centered compound stabilizes more charge on the aryl substituent away from the bridge, lowering H_{ab} and raising λ_s slightly and, hence, the ET rate constant by a rather modest amount, a factor of 2.5 at 260 K, although the slopes of the lines are different enough that the ratio calculated

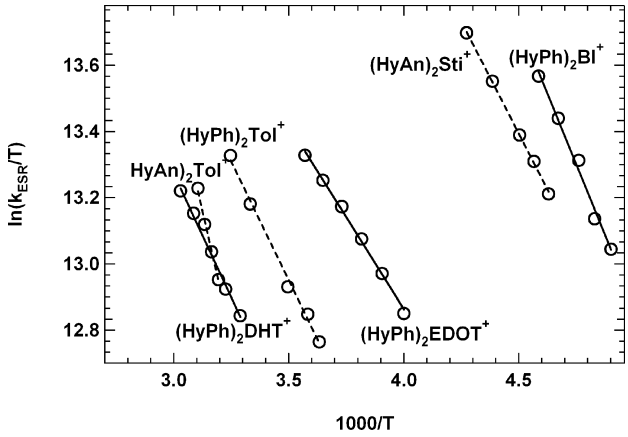

Figure 10. Eyring plots of ESR kinetic data. The solvent for the 11-bond bridged compounds is butyronitrile, that for the 13-bond bridged **(HyPh)$_2$DHT**$^+$ is 1,2-dichloroethane, and that for the 16-bond bridged **(HyPh)$_2$EDOT**$^+$ is methylene chloride.

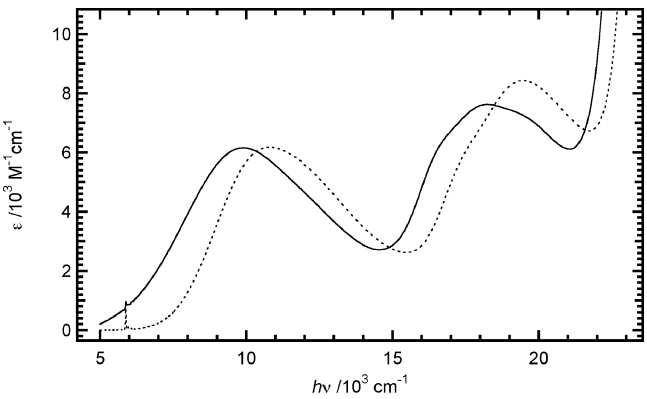

Figure 11. Comparison of optical spectrum of **(HyPh)$_2$EDOT**$^+$ (solid line) with the related monohydrazine radical cation **HyPhEDOT**$^+$ (broken line) in CH_2Cl_2.

depends upon temperature. The large deviation in $\Delta H^{\ddagger}$ for **(HyAn)$_2$Tol**$^+$ pointed out above is also obvious in Figure 10. Figure 10 also shows graphically the large rate difference between the 11-bond tolane and stilbene bridges; **(HyAn)$_2$Sti**$^+$ has a rate constant much closer to the 9-bond **(HyPh)$_2$BI**$^+$ than to the tolane.

Variable-temperature optical data were taken of butyronitrile for the compounds studied in this solvent and in 1,2-dichloroethane for **(HyPh)$_2$DHT**$^+$ to allow comparison of rate constants calculated from the optical spectra with those measured by ESR. Our experimental setup for obtaining variable-temperature optical spectra employs methanol circulating through a jacket cooling the optical cuvette and gives problems with water condensation below about −10 °C. Unfortunately **(HyAn)$_2$Sti**$^+$ proved to be too unstable at these higher temperatures that were used for the ESR kinetics to allow reliable optical parameters to be extracted. The spectrum of **(HyPh)$_2$EDOT**$^+$ is compared with that of its monohydrazine-substituted analogue in Figure 11. It may be seen that this 16-bond bridged compound has substantial overlap of the bis(hydrazine) radical cation and monohydrazine radical cation optical spectra; therefore, the contribution of the MV band for the bis(hydrazine) cannot be resolved, and meaningful optical rate constants cannot be calculated. The monohydrazine of the **DHT**-bridged system studied was not prepared, but the large shift of 3100 cm^{-1} between the lowest-energy absorption bands of **(HyPh)$_2$DHT**$^+$ in MC and AN (see Table 2) is evidence that the MV band is resolved for it (we note that the shift is only 700 cm^{-1} for the

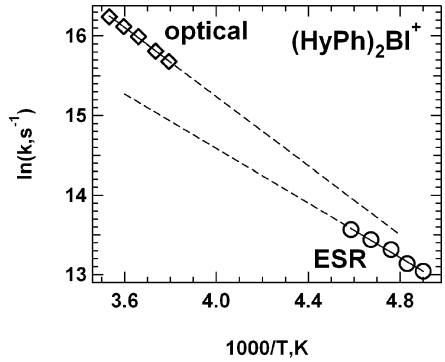

Figure 12. Comparison of Eyring plots for ESR data (circles) and optical data (diamonds) for **HyPh$_2$BI-d_{10}**$^+$.

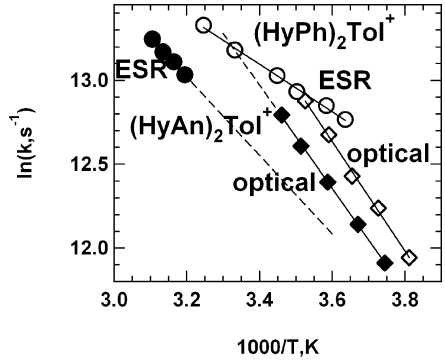

Figure 13. Comparison of Eyring plots for ESR data (circles) and optical data (diamonds) for **HyPh$_2$Tol-d_{18}**$^+$ (open symbols) and **HyAn$_2$Tol-d_8**$^+$ (filled symbols).

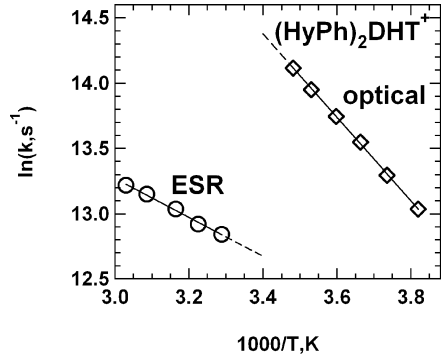

Figure 14. Comparison of Eyring plots for ESR data (circles) and optical data (diamonds) for **(HyPh)$_2$DHT**$^+$.

EDOT-bridged example). The rate constants for electron transfer were calculated from the parameters derived from the variable-temperature optical spectra as in our previous work,[5−10] and the results are shown pictorially in Figures 12−14. The electron transfer distance on the diabatic surfaces is required to extract H_{ab} from optical data. Here, we used values calculated on the adiabatic surfaces using AM1, which were converted to d_{ab} values using the optical spectra, as previously described.[43] The constants derived from the optical data have higher slopes than those produced from the ESR spectroscopy measurements, but the differences in predicted rate constants are not very large. The largest deviation is shown for the largest bridge, the 13-bond bridged **(HyPh)$_2$DHT**$^+$, and corresponds to a predicted optical rate constant that is a factor of 5.4 larger midway between the temperature ranges for which data are available, at 294 K. This is in the direction expected for the deviation from Hush theory as electron hopping became more important but is a rather small deviation. Unfortunately the 16-bond bridged

system **(HyPh)$_2$EDOT$^+$** has too much overlap of the bridge excitation and class II bands for a meaningful comparison of ESR with the optical rate constant; therefore, whether the ESR rate constant becomes less compatible with Hush theory as the bridge size is increased further and the bridge orbital/**M**$^+$-group orbital energy gap becomes smaller cannot be determined.

Conclusions

The 3-*tert*-butyl-substituted 2,3-diazabicyclo[2.2.2]bicyclooct-2-yl hydrazine charge-bearing unit (**HytBu**) that was used for obtaining ESR kinetics of intramolecular electron transfer within five- to nine-bond aryl-bridged mixed valence radical cations gave only slow electron-transfer limit ESR spectra when the number of bonds was increased above nine. To allow quantitative study, we replaced the *tert*-butyl groups with aryl groups, which allowed ESR kinetics for 9-, 11-, 13-, and 16-bond bridged systems to be obtained. It was necessary to deuterate the phenyl groups to get sharp enough ESR spectra for reasonably accurate rate constant simulation. The largest bridge for which good optical rate constant prediction were obtained was the 13-bond bridged system, **(HyPh)$_2$DHT$^+$**. It gave the largest deviation between optical and ESR rate constants found in this work, but the rate constant ratio was only a factor of 5.4 higher than the ESR rate constant extrapolated to 294 K compared to the extrapolated optical rate constant; therefore, effects of the expected breakdown of Marcus−Hush theory as the bridge size was increased were still rather small. An accurate optical rate constant could not be obtained for the larger 16-bond bridged system **(HyPh)$_2$EDOT$^+$** because of overlap in the optical spectrum of this compound.

Acknowledgment. We thank NSF for support of this work under CHE-0204197 and -0647719.

Supporting Information Available: ESR fitting parameters and comparison of calculated and experimental ESR spectra for the six **HyAr**-centered compounds in Table 7, estimation of electron-transfer distances, optical parameters used to calculate the rate constants shown in Figures 12−14, ion pairing data and plots, and details of compound preparation. This material is available free of charge via the Internet at http://pubs.acs.org.

References and Notes

(1) Robin, M. B.; Day, P. *Adv. Inorg. Radiochem.* **1967**, *10*, 247.
(2) Allen, G. C.; Hush, N. S. *Prog. Inorg. Chem.* **1967**, *8*, 357.
(3) Hush, N. S. *Prog. Inorg. Chem.* **1967**, *8*, 391.
(4) Nelsen, S. F.; Ismagilov, R. F.; Powell, D. R. *J. Am. Chem. Soc.* **1996**, *118*, 6313.
(5) Nelsen, S. F.; Ismagilov, R. F.; Powell, D. R. *J. Am. Chem. Soc.* **1997**, *119*, 10213.
(6) Nelsen, S. F.; Ismagilov, R. F.; Trieber, D. A., II. *Science* **1997**, *278*, 846.
(7) Nelsen, S. F.; Ismagilov, R. F.; Gentile, K. E.; Powell, D. R. *J. Am. Chem. Soc.* **1999**, *121*, 7108.
(8) Nelsen, S. F.; Ismagilov, R. F. *J. Phys. Chem. A* **1999**, *103*, 5373.
(9) Nelsen, S. F.; Trieber, D. A., II; Ismagilov, R. F.; Teki, Y. *J. Am. Chem. Soc.* **2001**, *123*, 5684.
(10) Nelsen, S. F.; Konradsson, A. E.; Teki, Y. *J. Am. Chem. Soc.* **2006**, *128*, 2902.
(11) For a review, see: Nelsen, S. F. *Adv. Phys. Org. Chem.* **2006**, *41*, 183.
(12) Nelsen, S. F.; Weaver, M. N.; Luo, Y.; Pladziewicz, J. R.; Ausman, L.; Jentzsch, T. L.; O'Konneck, J. J. *J. Phys. Chem. A* **2006**, *110*, 11665.
(13) Nelsen, S. F.; Schultz, K. P. submitted for publication.
(14) Lambert, C.; Nöll, G. *Angew. Chem., Int. Ed.* **1998**, *37*, 2107.
(15) Lambert, C.; Nöll, G. *J. Am. Chem. Soc.* **1999**, *121*, 8434.
(16) Barlow, S.; Risko, C.; Coropceanu, V.; Tucker, N. M.; Jones, S. C.; Levi, Z.; Khrustalev, V. N.; Antipin, M. Y.; Kinnibrugh, T. L.; Timofeeva, T.; Marder, S. R.; Brédas, J.-L. *Chem. Commun.* **2005**, 764.
(17) Barlow, S.; Risko, C.; Chung, S.-J.; Tucker, N. M.; Coropceanu, V.; Jones, S. C.; Levi, Z.; Brédas, J.-L.; Marder, S. R. *J. Am. Chem. Soc.* **2005**, *127*, 16900.
(18) Szeghalmi, A. V.; Erdmann, M.; Engel, V.; Schmidt, M.; Amthor, S.; Kriegisch, V.; Nöll, G.; Stahl, R.; Lambert, C.; Leusser, D.; Stalke, D.; Zabel, M.; Popp, J. *J. Am. Chem. Soc.* **2004**, *126*, 7834.
(19) Lambert, C.; Nöll, G. *J. Chem Soc., Perkin Trans. 2* **2002**, 2039.
(20) Nelsen, S. F.; Ismagilov, R. F.; Powell, D. R. *J. Am. Chem. Soc.* **1998**, *120*, 1924.
(21) Bell, F. A.; Ledwith, A.; Sherring, D. C. *J. Chem. Soc. C* **1969**, 2719.
(22) Connelly, N. G.; Geiger, W. E. *Chem. Rev.* **1996**, *96*, 877.
(23) Waybright, S. M.; McAlpine, K.; Laskoski, M.; Smith, M. D.; Bunz, U. H. F. *J. Am. Chem. Soc.* **2002**, *124*, 8661.
(24) Liu, Z. Q.; Fang, Q.; Cao, D. X.; Wang, D.; Xu, G. B. *Org. Lett.* **2004**, *6*, 2933.
(25) Jeong, K. S.; Kim, Y. S.; Kim, Y. J.; Lee, E.; Yoon, J. H.; Park, W. H.; Park, Y. W.; Jeon, S. J.; Kim, Z. H.; Kim, J.; Jeong, N. L. *Ang. Chem., Int. Ed.* **2006**, *45*, 8134.
(26) Maruyama, S.; Kawanisni, Y. *J. Mater. Chem.* **2002**, *12*, 2245.
(27) Zhou, C. Z.; Liu, T. X.; Xu, J. M.; Chen, Z. K. *Macromolecules* **2003**, *36*, 1457.
(28) Zhao, X. Y.; Pinto, M. R.; Hardison, L. M.; Miwaura, J.; Muller, J.; Jiang, H.; Witker, D.; Kleiman, V. D.; Reynolds, J. R.; Schanze, K. S. *Macromolecules* **2006**, *39*, 6355.
(29) Xue, C. H.; Luo, F. T. *Tetrahedron* **2004**, *50*, 6285.
(30) Blomgren, F.; Larsson, S.; Nelsen, S. F. *J. Comput. Chem.* **2001**, *22*, 655.
(31) Nelsen, S. F.; Blackstock, S. C.; Kim, Y. *J. Am. Chem. Soc.* **1987**, *109*, 677.
(32) Creutz, C. *Prog. Inorg. Chem.* **1983**, *30*, 1–73.
(33) Nelsen, S. F.; Weaver, M. N.; Zink, J. I.; Telo, J. P. *J. Am. Chem. Soc.* **2005**, *127*, 10611.
(34) Nelsen, S. F.; Weaver, M. N.; Luo, Y.; Lockard, J. V.; Zink, J. I. *Chem. Phys.* **2006**, *324*, 195.
(35) Nelsen, S. F.; Luo, Y.; Weaver, M. N.; Lockard, J. V.; Zink, J. I. *J. Org. Chem.* **2006**, *71*, 4286.
(36) Valverde-Aguilar, G.; Wang, X.; Plummer, E.; Lockard, J. V.; Zink, J. I.; Nelsen, S. F.; Luo, Y.; Weaver, M. N. *J. Phys. Chem. A* **2008**, *112*, 7332.
(37) Nelsen, S. F.; Ismagilov, R. F. *J. Phys. Chem. A* **1999**, *103*, 5373.
(38) Nelsen, S. F.; Konradsson, A. E.; Teki, Y. *J. Am. Chem. Soc.* **2006**, *128*, 2902.
(39) Trieber, D. A., II. Ph.D. Thesis, University of Wisconsin, Madison, WI, 2000.
(40) Grampp, G.; Shohoji, M. C. B. L.; Herold, B. J. *Ber. Bunsen-Ges. Phys. Chem.* **1989**, *93*, 580.
(41) Telo, J. P.; Shohoji, M. C. B. L. *J. Chem. Soc., Perkin Trans. 2* **1998**, 711.
(42) Telo, J P.; Grampp, G.; Shohoji, M C. B. L. *Phys. Chem. Chem. Phys.* **1999**, *1*, 99.
(43) Nelsen, S. F.; Newton, M. D. *J. Phys. Chem. A* **2000**, *104*, 10023. Although there is a slight dependence of the dab value obtained upon which the diasteromer is calculated (Nelsen, S. F.; Blomgren, F. *J. Org. Chem.* **2001**, *66*, 6551.), the differences are not significant compared to the accuracy of the analysis, and we only looked at one diasteromer here.

JP811433P